Journal of Membrane Science 368 (2011) 95–99

Contents lists available at ScienceDirect

Journal of Membrane Science

journal homepage: www.elsevier.com/locate/memsci

Application of high speed imaging as a novel tool to study particle dynamics in tubular membrane systems

Ralph Lindeboom[a], Geo Smith[b], David Jeison[c], Hardy Temmink[a], Jules B. van Lier[d,*]

[a] Sub-Department of Environmental Technology, Wageningen University, P.O. Box 8129, 6700 EV Wageningen, The Netherlands
[b] Norit Process Technology BV, P.O. Box 741, 7500 AS Enschede, The Netherlands
[c] Chemical Engineering Department, Universidad de La Frontera, Casilla 54-D, Temuco, Chile
[d] Delft University of Technology, Faculty of Civil Engineering and Geosciences, Department of Water Management, Section Sanitary Engineering, P.O. Box 5048, 2600 GA Delft, The Netherlands

ARTICLE INFO

Article history:
Received 10 March 2010
Received in revised form 9 August 2010
Accepted 11 November 2010
Available online 19 November 2010

Keywords:
High speed video
MBR
Membrane
Slug flow

ABSTRACT

Membrane bioreactors represent a promising technology for wastewater treatment, already applied to a wide variety of industrial effluents and sewage. Gas or air sparging is a commonly applied approach to generate surface shear to control fouling phenomena and cake formation causing flux reduction. In inside-out tubular membranes, gas sparging is usually applied to promote the development of a slug flow regime. Our present paper describes the development of a novel technique to study particle dynamics in tubular systems under slug flow regime. It combines the use of a laser beam generator to illuminate model particles, which are then motion pictured by means of a high speed camera. Digital video analysis is subsequently used to follow and study particle movements. The presented technique can be combined with other approaches such as CFD analysis in order to advance in the understanding of particle dynamics in tubular membrane systems.

1. Introduction

Membrane filtration has been successfully applied to biological wastewater treatment for over one decade. The integration of membrane filtration with a biological reactor, creating a membrane bioreactor (MBR), represents a reliable way to provide biomass retention, and to achieve high quality treated water. Flux reduction due to membrane fouling and particle deposition remains the main limiting factor for the application of MBRs. Even though extensive research has been conducted in this field, fouling phenomena are still far from fully understood and characterized, due to the complex interactions existing between the different fouling parameters [1]. Particle deposition over the membrane surface is definitely one of the main flux-reducing phenomena, since cake layer formation can substantial increase filtration resistance. Indeed, cake layer formation has been identified as a determining phenomenon for the applicable flux in both aerobic and anaerobic MBRs for wastewater treatment [2–4].

Particle deposition is determined by the balance of convective transport and back-transport. Shear induced diffusion is the predominant back-transport mechanism during microfiltration of suspensions with particles in the range 0.5–30 μm [5], and is directly related with the applied shear at the membrane surface, dependent on the operational conditions. Many authors have recognized gas sparging as an efficient tool for providing membrane shear and therefore flux enhancement [6–8], for both submerged and side-stream configurations. The injection of gas in inside-out tubular membranes has received increasing attention as a way to control particle deposition. When bubble sizes approaches that of the tube diameter, characteristic bullet-shaped bubbles are formed, referred to as slugs or Taylor bubbles. The formation of gas slugs inside tubular inside-out membranes enhances permeate fluxes by generating wall shear stress that disrupts the boundary layer and controls cake layer formation [8–10].

The impact of gas slug flow on hydrodynamics has been described in literature (e.g. [11–13]). Computational fluid dynamics (CFD) have been previously applied to study two-phase flow in inside-out tubular membranes [8]. However, validation of such models is sometimes difficult due to the complexity of real systems: wide range of particle sizes, particle interaction, and non-Newtonian rheology. The present paper describes a novel approach to study particle dynamics in systems working under slug flow regime, like inside-out tubular membranes. The presented novel methodology uses high speed imaging, combined with particle

* Corresponding author at: Delft University of Technology, Faculty of Civil Engineering and Geosciences, Department of Water Management, Section Sanitary Engineering, P.O. Box 5048, 2600 GA Delft, The Netherlands. Tel.: +31 0 15 27 81615; fax: +31 0 15 27 84918; mobile: +31 0 624996762.
E-mail address: j.b.vanlier@tudelft.nl (J.B. van Lier).
URL: http://www.watermanagement.tudelft.nl (J.B. van Lier).

0376-7388/$ – see front matter © 2010 Elsevier B.V. All rights reserved.
doi:10.1016/j.memsci.2010.11.029

image velocimetric analysis (PIV), to directly observe and measure the movement of model particles. Information acquired by this technique can be of great utility for validating CFD modelling and to understand the effect of different flow characteristics over particle dynamics.

2. Materials and methods

A schematic representation of the used setup is presented in Fig. 1. A 5 mm diameter glass tube was used as a model for an inside-out tubular membrane. A slug flow regime was induced inside the tube, using air and a suspension of model particles. The glass tube was positioned vertically, connected with two vessels, one at the bottom and one on the top. Air was injected inside the tube by means of a peristaltic pump (Watson Marlow 323), originating a gas lift effect that induced suspension circulation from bottom to top vessels. A tube connecting both vessels allowed the return of the suspension from top to bottom, so the setup could be operated continuously.

A continuous Argon ion laser (maximum power 2 W, Coherent Innova 90) was located one meter away from the glass tube. A 400 mm (focal length) plan-convex and a 63 mm (focal length) pan-cylindrical lens were used to generate a light sheet from the laser beam generator into the glass tube. In the filming area, the light sheet was 25 mm wide and 0.2 mm thick. Laser light was reflected by the particles contained in the suspension towards a high speed camera positioned at a 90° angle with respect of the laser beam generator. The camera, Redlake Motionpro 3000 with a Nikon Micro Lens (105 mm 2.8, f stop 5.6, with a 27.5 mm extension ring), was placed at a distance of 12 cm from the glass tube. Digital video was acquired at a frame rate of 1600 frames per second, at an optical resolution of 1000 pixels/cm. At the glass tube position where the high speed camera observation was performed, a water filled cubic glass cuvette with sides of 5 cm was placed around the tube, in order to correct the refraction index. Two test suspensions were prepared, by mixing demineralised water with either 6 μm Nylon beads (density 1.15 g/cm^3), and 50–100 μm white PVC particles (density 1.4 g/cm^3). Both suspensions were prepared at a concentration of 5 g/l. The selection of the model particles was made based on reflectivity, size and density. To enhance observation, the whole setup was placed in a dark room.

Actual bubble sizes and distances were determined by a calibration process involving acquisition of images of objects of known dimensions.

Gas was injected by means of a nozzle in the bottom vessel. In order to provide different slug sizes, 3 different gas nozzles were used: 3, 5, and 7 mm of diameter. During the experiments, the gas flow rate was modified resulting in bubble velocities (actual rising velocity) between 0.3 and 1.5 m/s.

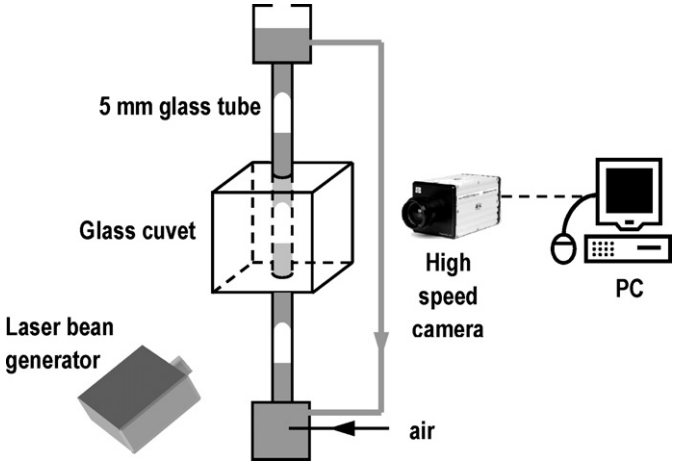

Fig. 1. Schematic overview of the high speed imaging setup.

Table 1
Slug flow characteristics determined by image analysis.

Amount	Units	Description
Bubble velocity (BV)	m/s	Actual bubble rising velocity (not the superficial gas velocity[a])
Bubble length (BL)	mm	Length of the bubble, from head to tail
Void fraction	%	Length of the gas slug (bubble) divided by the sum of the lengths of the liquid and gas slug
Turbulence fraction	%	Length of the turbulent zone divided by the sum of the lengths of liquid and gas slugs. Turbulent zone is defined as that part of the liquid slug where the velocity vectors of the particles are not in parallel to the tube wall
Frequency	1/min	Number of bubbles passing by the observed zone of the glass tube per minute
Particle counts		Amount of particles in the liquid slug behind each gas slug
Particle bulk velocity	m/s	Vertical velocity (in parallel to bubble velocity) of particles contained in the liquid slug
Particle wall velocity	m/s	Velocity of particles contained between the bubble and the glass tube wall. A positive value means an upward velocity, in the same direction as the liquid and gas flow. A negative velocity value means a downward velocity, in the opposite direction of the flow

[a] Superficial velocity is evaluated as the gas flow divided by the glass tube transversal area.

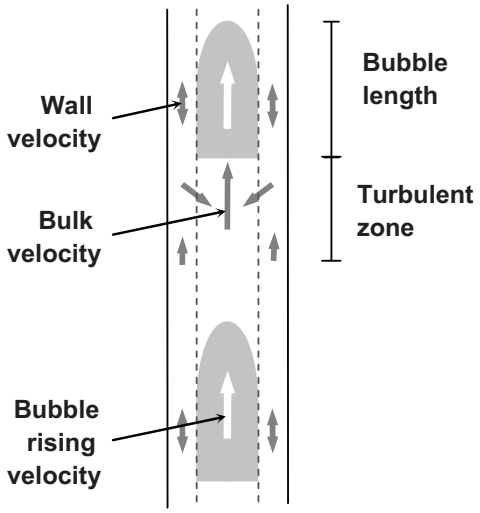

Fig. 2. Diagram representing some of the quantities defined in Table 1 for characterizing slug flow regime.

Several parameters were used to characterize the slug flow regime. These are defined in Table 1. Some of them are also schematically represented in Fig. 2. Measurements were performed using MiDAS player (Xcitex Inc., USA) and DLT Data Viewer 2 (a Matlab module developed by Ty Hedrick, http://www.unc.edu/~thedrick). All reported values used for characterization of the slug flows are averages over at least 10 gas slugs.

3. Results and discussion

Fig. 3 presents pictures from typical rising slugs obtained by means of the described setup. Gas slugs dimensions, shape and velocity can be easily determined by image and video analysis. Particles can be clearly observed and their movement followed, so

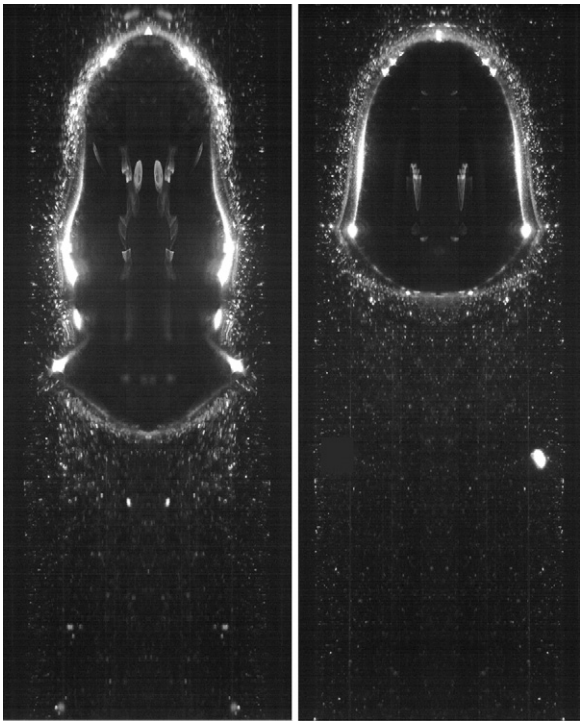

Fig. 3. Pictures of a rising gas slug. Particle sizes used were 6 μm (Nylon beads) and 50–100 μm (PVC beads).

characteristics described in Table 1 can be evaluated by means of digital video analysis.

Table 2 presents pictures of typical bubble shapes observed at the different conditions tested, along with the slug flow pattern characteristics defined in Table 1. Data clearly shows that the way the bubble is introduced into the tube is highly significant for the characteristics of the gas slug. Bubble length showed to be positively correlated with the size of applied nozzles. For each of the nozzle sizes, longer gas slugs are observed when the gas flow is increased. In turn, longer gas slugs are obtained when the gas flow is increased. It has to be noticed that the actual rising bubble velocity is also determined by the liquid flow generated by the gas-lift effect, eventually leading to gas–liquid flow equilibrium. Bubbles frequency also shows to be dependent on the gas flow and nozzle diameter. For a given nozzle diameter, more bubbles will be produced when more gas is introduced in the tube. Since an increase in nozzle size produces bigger bubbles, bubble frequency reduces, for a given gas flow. Pictures included in Table 2 also show how different conditions generate different nose and especially tail shapes, ranging from a steady form with multiple tail waves, to unsteady shapes. Bubbles shapes obtained with 3 and 5 mm nozzles are visually similar to those bubbles described by [14].

Turbulent fraction, as defined in Table 1, is certainly related to mass transport phenomena, factor of crucial importance for reducing particle deposition during membrane filtration operations. Results presented in Table 2 show that the applied gas flow had a clear impact on the turbulence fraction, for the 3 nozzle sizes tested. Such relation is likely the result of the positive effect of gas flow over bubble size and velocity. Lower gas flows resulted in short wakes behind a bubble, which are immediately followed by a turbulence-free region that lasts until the nose region in front of the next bubble. On the contrary, at high gas flows (128 and 256 ml/min), a turbulent regime was observed from the bubble tail to the nose of the next bubble. Even though longer turbulent fractions are obtained when longer bubbles are induced, this does not mean that this condition is desirable for increasing filtration flux. Actually, previous studies indicate that shorter gas slugs were found to be better for flux enhancement [9], since the turbulence caused by the annular film impinging the liquid slug behind the bubble plays a pivotal role in transfer augmentation [15], whereas the film regions, adjacent to the gas slugs, induce a low shear [9]. An optimum condition for filtration would be then to induce turbulent conditions to a maximum fraction of the liquid phase. Our current setup enabled a qualitative definition of turbulence (Table 1). No quantitative determination of the degree of turbulence was possible at this time. Therefore, even though we expect that a maximum fraction of liquid turbulence is required for cake layer removal, more in-depth study on quantification of the turbulence in the liquid slug will be required.

Application of high speed imaging can be used to follow individual particle movements. However, it has to be remarked that measurements are performed over a two-dimensional flat plane were images are acquired. Therefore, particle tracking was only possible in 2 dimensions, those perpendicular to the camera

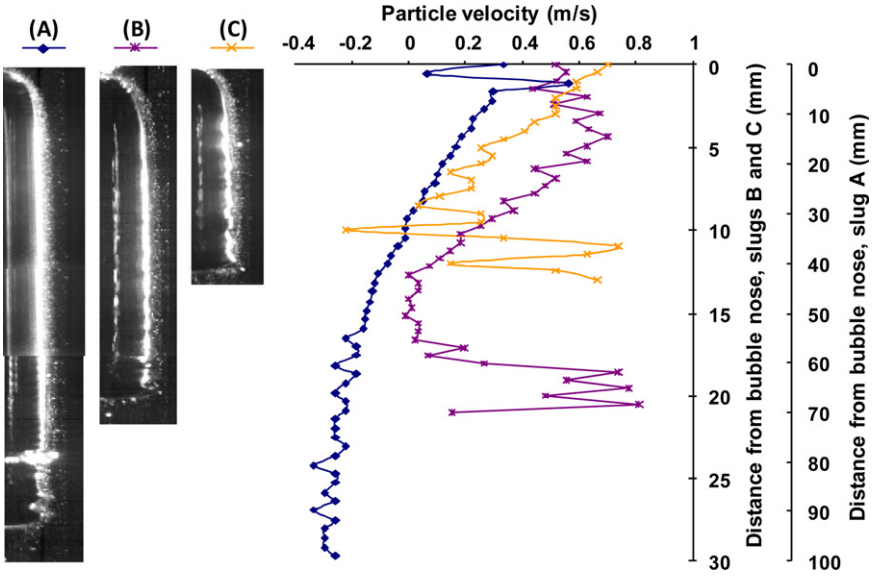

Fig. 4. Typical particle velocities between a gas slug and a glass tube wall, for 3 different gas slugs. (A) 7 mm nozzle, BV 1.28 m/s, BL 99 mm; (B) 5 mm nozzle, BV 1.24 m/s, BL 21 mm; (C) 3 mm BV 1.1 m/s BL 13 mm. Model particles: white PVC particles.

Table 2
Slug flow characterization from high speed video analysis by particle image velocimetry (6 μM Nylon beads), at different operational conditions: nozzle diameter and gas flow.

Nozzle diameter, gas flow	Typical bubble shape[a]	Bubble velocity (m/s)	Avg. bubble length (cm)	Void fraction (%)	Turbulence fraction (%)	Frequency (1000/min)	Particle bulk velocity[b] (m/s)	Particle wall velocity[b] (m/s)
3 mm, 32 ml/min	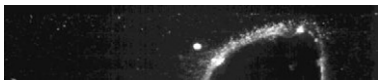	0.38	0.47	0.23	0.25	1.08	0.50	0.05
3 mm, 64 ml/min	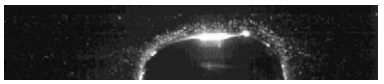	0.35	0.54	0.28	0.40	1.03	0.42	0.04
3 mm, 128 ml/min	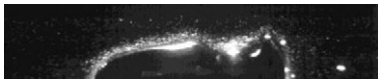	0.81	0.85	0.37	0.52	2.09	0.86	0.10
3 mm, 256 ml/min	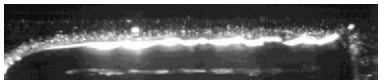	1.03	1.16	0.46	0.54	2.44	1.18	0.13
5 mm, 32 ml/min	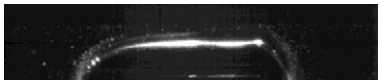	0.37	0.99	0.42	0.18	0.88	0.39	0.09
5 mm, 64 ml/min	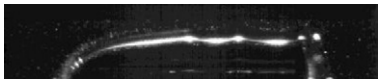	0.57	0.97	0.33	0.26	1.15	0.64	0.07
5 mm, 128 ml/min	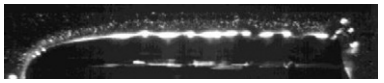	0.78	1.16	0.34	0.42	1.31	0.86	0.09
5 mm, 256 ml/min	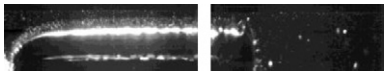	1.12	1.51	0.42	0.58	1.98	1.19	0.17
7 mm, 32 ml/min	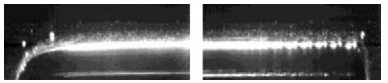	0.80	4.91	0.49	0.29	0.08	1.18	0.09
7 mm, 64 ml/min	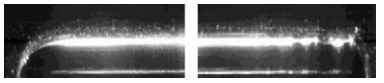	0.39	6.17	0.25	0.09	0.09	0.61	0.08
7 mm, 128 ml/min	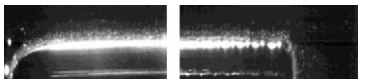	0.94	9.08	0.27	0.28	0.20	1.06	0.14
7 mm, 256 ml/min	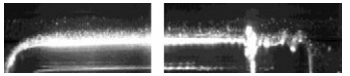	1.25	10.0	0.36	0.64	0.41	1.27	0.13

[a] Some images are cut since gas slugs where to long to be captured in a single frame at the chosen optical zoom. In those cases images of the head and tail sections are presented.
[b] Particle velocities are evaluated with respect to a fixed observer (not relative to the liquid velocity).

position. Research is currently being performed to improve this method further, including the horizontal particle velocity in the measurements. Despite this limitation, velocity profiles can be evaluated for example for the liquid film located between the tube wall and the gas slug, where particle movement is expected to be mainly one-dimensional, i.e. vertical in the direction parallel to the tube. Fig. 4 presents typical determinations, for 3 different conditions. Vertical particle velocity is presented as a function of the particle position, expressed as the distance from the bubble nose. The proposed methodology is able to quantify the differences in the vertical particle velocities between particles exposed to different conditions. It has to be reminded that reported velocities are with respect to a fixed observer. So, in order to have relative velocities with respect to the actual liquid velocity, the values need to be corrected. Particle velocities reported in Fig. 4 have a precision of 0.02 m/s for the region between the bubble and tube wall, and 0.05 m/s for the region adjacent to the bubble nose and tail. Of interest is the observation that long gas slugs (slug A) result in negative particle velocities, leading to downward movements (Fig. 4). Consequently, particles stay in the test tube.

The proposed method is based on image acquisition, using a glass tube as a model for the membrane tube. Therefore, data are obtained in a non-filtrating system, and thus the effect of convective transport towards the membrane surface due to permeate collection is not included in the measurement. Since filtrating conditions can actually be considered or not during CFD modelling, the here presented technique is anyway of great value for calibrating or validating such models.

Our results clearly show that by using the developed high speed imaging tool, valuable information regarding the characteristics of slug flow regimes and individual particle movement can be obtained. Some of the parameter presented in Table 1 can be used to evaluate the effect of different operating conditions. At the same time, the method provides useful data for validation of CFD models. Even though the presented technique has limitations, as already discussed, it provides useful information on particle dynamics that can be used as a validation tool for dynamic models or to provide insight on particle behaviour during membrane filtration operations.

4. Conclusion

High speed imaging represents a useful tool to visualize particle dynamics in fluid flowing suspensions. It provides information on individual particle movements that may be used for validation or parameter estimation of CFD or other types of modelling involving suspensions. It can also provide information useful for establishing relations between operational conditions and characteristics of slug flow regime, such as bubble speed, dimensions and shape. Such information could be of great value when studying particle deposition in membrane systems, since this phenomenon is one of the main factors determining flux reduction when concentrated suspensions needs to be filtrated, as is the case of membrane bioreactors for wastewater treatment.

Acknowledgements

Authors would want to thank Jos van de Boogaart, Chairgroup of Experimental Zoology, for his help with the high speed camera experimental setup. David Jeison acknowledges the support provided by FONDECYT Project 1080279 (CONICYT, Chile).

References

[1] P. Le-Clech, V. Chen, T.A.G. Fane, Review: fouling in membrane bioreactors used in wastewater treatment, J. Membr. Sci. 284 (2006) 17–53.
[2] J. Lee, W.Y. Ahn, C.H. Lee, Comparison of the filtration characteristics between attached and suspended growth microorganisms in submerged membrane bioreactor, Water Res. 35 (2001) 2435–2445.
[3] F. Meng, F. Yang, Fouling mechanisms of deflocculated sludge, normal sludge, and bulking sludge in membrane bioreactor, J. Membr. Sci. 305 (2007) 48–56.
[4] D. Jeison, J.B. van Lier, Cake formation and consolidation: main factors governing the applicable flux in anaerobic submerged membrane bioreactors (AnSMBR) treating acidified wastewaters, Sep. Purif. Technol. 56 (2007) 71–78.
[5] G. Belfort, R.H. Davis, A.L. Zydney, The behavior of suspensions and macromolecular solutions in cross-flow microfiltration, J. Membr. Sci. 96 (1994) 1–58.
[6] S.R. Smith, Z.F. Cui, R.W. Field, Upper and lower-bound estimates of flux for pas sparged ultrafiltration membranes with hollow fiber membranes, Ind. Eng. Res. 44 (2004) 7684–7695.
[7] P.R. Bérubé, E.R. Hall, P.M. Sutton, Parameter governing permeate flux in an anaerobic membrane bioreactor treating low strength municipal wastewaters: a literature review, state-of-the-review, Water Environ. Res. 78 (2006) 887–896.
[8] Z.F. Cui, S. Chang, A.G. Fane, The use of gas bubbling to enhance membrane processes, J. Membr. Sci. 221 (2003) 1–35.
[9] S.R. Smith, Z.F. Cui, Gas-slug enhanced hollow fibre ultrafiltration—an experimental study, J. Membr. Sci. 242 (2004) 117–128.
[10] T. Taha, Z.F. Cui, CFD modeling of gas-sparged ultrafiltration in tubular membranes, J. Membr. Sci. 210 (2002) 13–27.
[11] V.E. Nakoryakov, O.N. Kashinsky, A.P. Burdukov, V.P. Odnoral, Local characteristics of upward gas liquid flows, Int. J. Muhiphase Flow 7 (1981) 63–81.
[12] S. Laborie, C. Cabassud, Modeling and measurement of shear stress for a slug flow inside a capillary, AIChE J. 51 (2005) 1104–1115.
[13] C.C.V. Chan, P.R. Bérubé, E.R. Hall, Shear profiles inside gas sparged submerged hollow fiber membrane modules, J. Membr. Sci. (2007) 104–120.
[14] D. Zheng, X. He, D. Che, CFD simulations of hydrodynamic characteristics in a gas–liquid vertical upward slug flow, Int. J. Heat Mass Transfer 50 (2007) 4151–4165.
[15] T. Taha, Z.F. Cui, CFD modelling of slug flow in vertical tubes, Chem. Eng. Sci. 61 (2006) 676–687.